DRAFT VERSION NOVEMBER 6, 2018
Typeset using LaTeX **modern** style in AASTeX62

HERA Memo 55: Bispectrum Phase Delay Spectrum Analysis and Diagnostics

J. KENT,[1] B. NIKOLIC,[1] C. L. CARILLI,[2,1] N. THYAGARAJAN,[2] K. GALE-SIDES,[1]
SIYANDA MATIKA,[3,4] AND GIANNI BERNARDI[3,4,5]

[1]*Astrophysics Group, Cavendish Laboratory, University of Cambridge, UK*
[2]*National Radio Astronomy Observatory, P. O. Box 0, Socorro, NM 87801*
[3]*Rhodes University, South Africa*
[4]*Square Kilometre Array South Africa*
[5]*INAF-IRA, Italy*

1. INTRODUCTION

The closure phase has shown potential as a strategy for separating out the HI spin flip transition from foregrounds during the reionisation epoch using the delay spectrum technique (Thyagarajan et al. 2018; Carilli & Sims 2016).

This memo describes initial work in producing delay spectra using the closure phases, also known as the bispectrum, of redundant triads of antennas.

Here we look at how the delay spectra vary across different redundant triads groups, polarisations, and the frequency band that is delay transformed. The results are varied and complex however some definitive trends emerge.

2. DATA AND PROCESS

All of the data used in this memo is from the HERA IDR2.1 data release (Dillon & Team 2018). The time span is centred on the transit of Fornax-A (RA = $03^{h}22^{m}42^{s}$, Dec = $-37^{\circ}12'30''$). Each closure record corresponds to 10.7s of integrated data. The LST range in use for this analysis is $02^{h}45^{m}00^{s}$ to $03^{h}56^{h}00^{s}$. This is where the closure spectra of triads of the same geometry converge with respect to each other.

The triads studied are equilateral 14m (EQ14), equilateral 28m (EQ28), East-West (LinEW), and $\pm 30^{\circ}$ (LinP30/LinM30) with respect to the north.

The data used to generate the closure phases was raw visibility data, with no calibration applied. The properties of the closure is such that antenna based direction-independent calibration effects should cancel out, provided there are no closure errors.

The closure phases are projected onto the unit circle as a complex quantity and the delay spectrum taken:

$$C = e^{i\phi} \tag{1}$$

Where ϕ is the closure phase, and C is the closure phase after projection onto the unit circle. Then the delay spectrum is taken by Fourier transforming the closure spectra:

$$\hat{D}(\tau) = \mathscr{F}\left[C(f)\right] \quad (2)$$

From this, we can infer a direct signal to noise ratio measurement on the closures using the delay spectrum technique. Firstly cross-correlation is done between different the medians of two separate sets of days in IDR2.1, $\hat{C}_a = Median\{d_0 \ldots d_8\}$ $\hat{C}_b = Median\{d_9 \ldots d_{18}\}$, where d_i represents a particular day in our dataset. We compute the cross spectral density, where one delay spectrum is multiplied by the conjugate of another:

$$\bar{D}_{ab}(\tau) = \hat{D}_a(\tau)\hat{D}_b^*(\tau) \quad (3)$$

$\bar{D}$ represents the cross-correlated spectra. Averaging, both coherently(before the delay transform) over 2-4 records, and incoherently (after the delay transform) over different triads and over the entire LST range,increases the dynamic range by reducing noise further by $\frac{1}{\sqrt{N}}$. In the figures in this memo, only incoherent averaging has been performed.

3. ANALYSIS AND RESULTS

Our plots take a median across two blocks of 9 days each, of the 18 days in the IDR2.1 dataset, for each 10,7 second record [1]. The median filtering helps negate the effect of RFI. Then the delay spectrum is taken of both of these blocks and they are cross-correlated with each other, giving $N_{\text{triads}} \times N_{\text{records}}$ of delay spectra. These are then averaged together incoherently to reduce noise further. The delay spectra of EQ14 and EQ28 triads are shown in Figures 1 and 2 for the lower and upper channel band, respectively. The lower channel band is from 111.7 MHz to 137.1 MHz, and the upper band from 150.3Mhz to 175.7MHz. The delay spectra for the LinEW, LinP30 and LinM30 triad classes are shown in Figures 3 and 4.

The 1μs ripple from the cable reflections is very visible in all delay spectra. This suggests that either the reflection is coming in as a additive (baseline-dependent) term, although leakage of a stronger (antenna-based gain) term cannot be ruled-out. Other trends emerge such as the consistently better dynamic range of YY polarisations over XX.

Averaging incoherently over time yields a noise reduction in high delay modes of an expected $\frac{1}{\sqrt{N}}$, as demonstrated in Figure 5, with N = 100.

Averaging over all triads is shown in Figure 6, which further reduces the noise floor. It does not reduce as $\frac{1}{\sqrt{N}}$ (N = 30) due to some shared baselines shared between different triads, and hence some fraction of the noise becomes common across triads. However, the systematic structure across the delay spectrum appears less pronounced after triad averaging.

Flagging represents another area where care has to be taken with how it is accounted for in generating the final power spectrum. The simplest method is to set a channel to zero, however this can introduce sharp impulses to the signal.

[1] Our analysis code can be found at https://github.com/HERA-Team/ClosurePS.

Figure 7 shows an example of the worst case flagging strategy, where a channel is set to zero if it is flagged. The resulting power spectrum loses a significant amount of dynamic range due to the sharp impulse of the flagged channel causing harmonics to distribute power across all delays, and raising our noise significantly.

Note that for the previous power spectra, no flagging was employed. The closure phase spectra for the frequency ranges chosen, after LST binning, are completely free of RFI (Nikolic et al. 2018).

4. SUMMARY

Delay spectra have been presented for the closure spectrum for various triad classes for XX and YY polarisations and in two sub-bands of the HERA band for different classes of triads. Averaging incoherently over both 600 seconds of closure records and all triads of the same geometry resulted in an increase in the signal to noise ratio, which broadly agrees with statistical theory.

Using YY polarisation and with averaging over 100 records (600 seconds) in the Fornax-A field, a dynamic range of 1 part in 10^8 was achieved, compared to the 1 part in 10^9 for the HI signal prescribed by the Bispectrum simulations Thyagarajan et al. (2018). Why YY polarisations and the lower band chosen is superior to other configurations is unclear, with investigations ongoing.

REFERENCES

Carilli, C., & Sims, P. 2016, HERA Mock Observations: Looking for Closure HERA Memorandum Number 13, HERA Project Memorandum 13, HERA Collaboration

Dillon, J., & Team, H. A. 2018, Internal Data Release 2.1, HERA Project Memorandum 45, HERA Collaboration

Nikolic, B., Carilli, C., & Kent, J. 2018, HERA Memo 54 Bispectrum Phase around Fornax A Transit using IDR2.1 Data, HERA Project Memorandum 54, HERA Collaboration

Thyagarajan, N., Carilli, C. L., & Nikolic, B. 2018, Physical Review Letters, 120, 251301

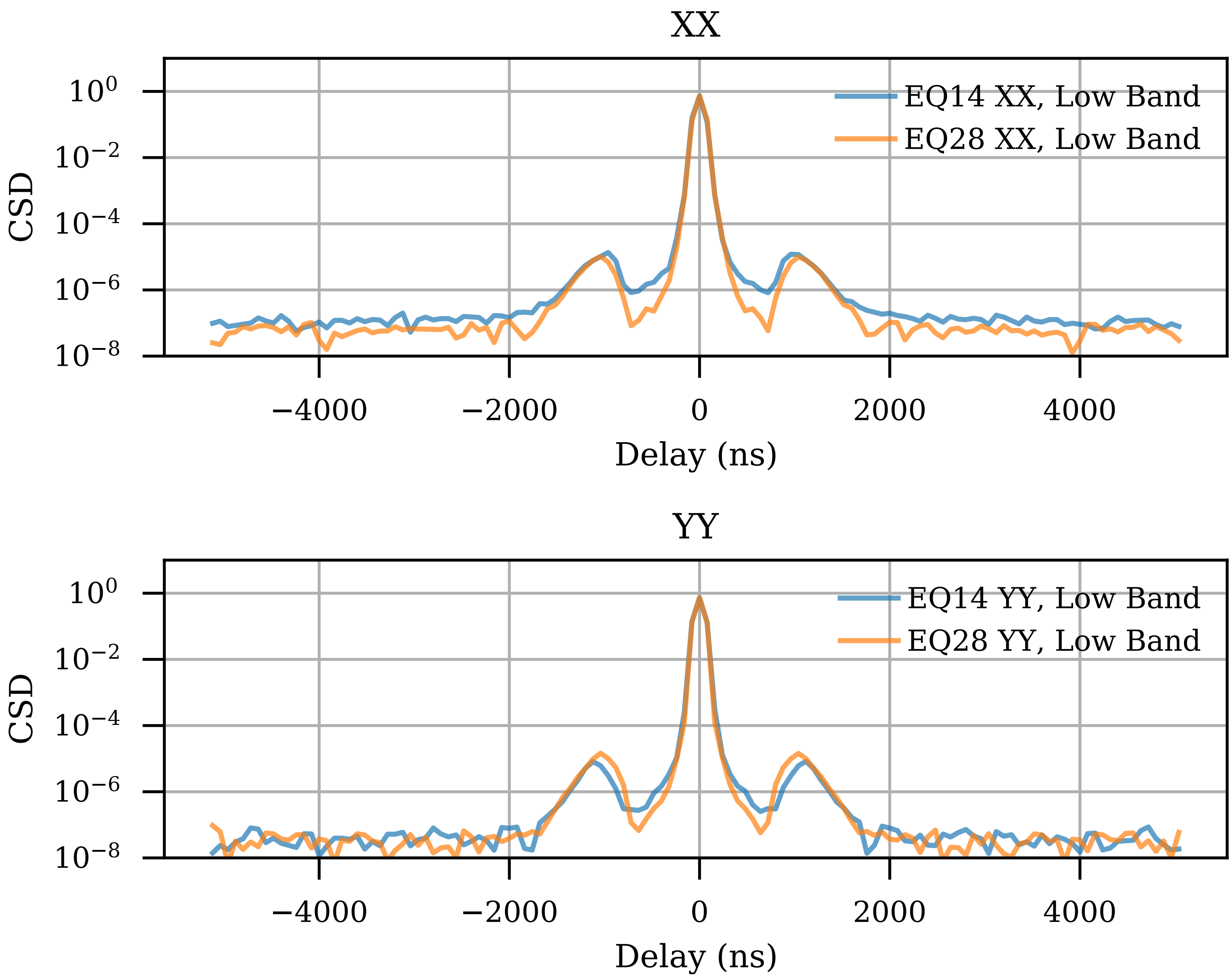

Figure 1: Delay transform of equilateral triads over a frequency band of 115-138MHz. CSD is the cross spectral power density, normalised on the unit circle.

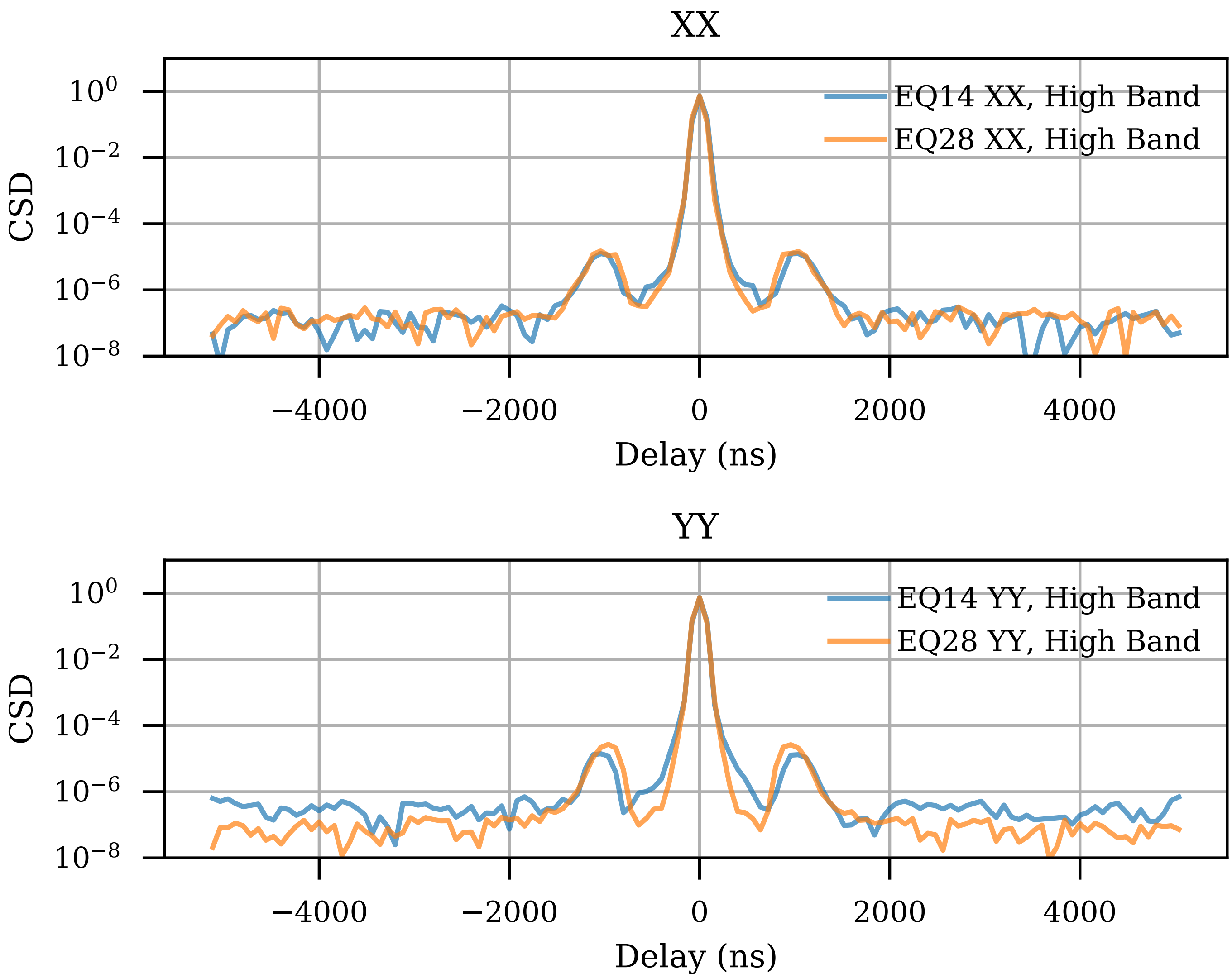

Figure 2: Delay transform of equilateral triads over a frequency band of 150-175MHz. CSD is the cross spectral power density, normalised on the unit circle.

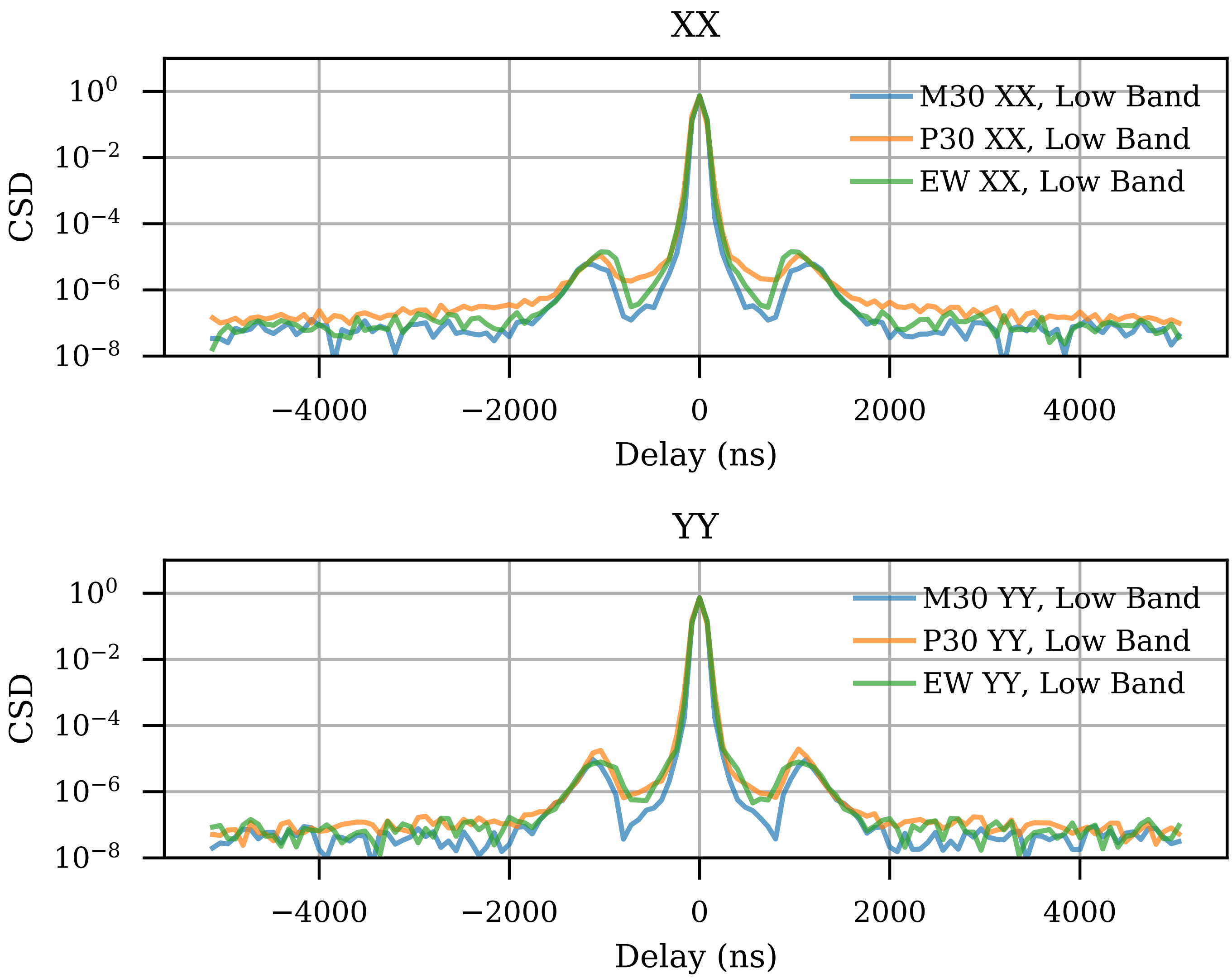

Figure 3: Delay transform of linear triads over a frequency band of 115-138MHz. CSD is the cross spectral power density, normalised on the unit circle.

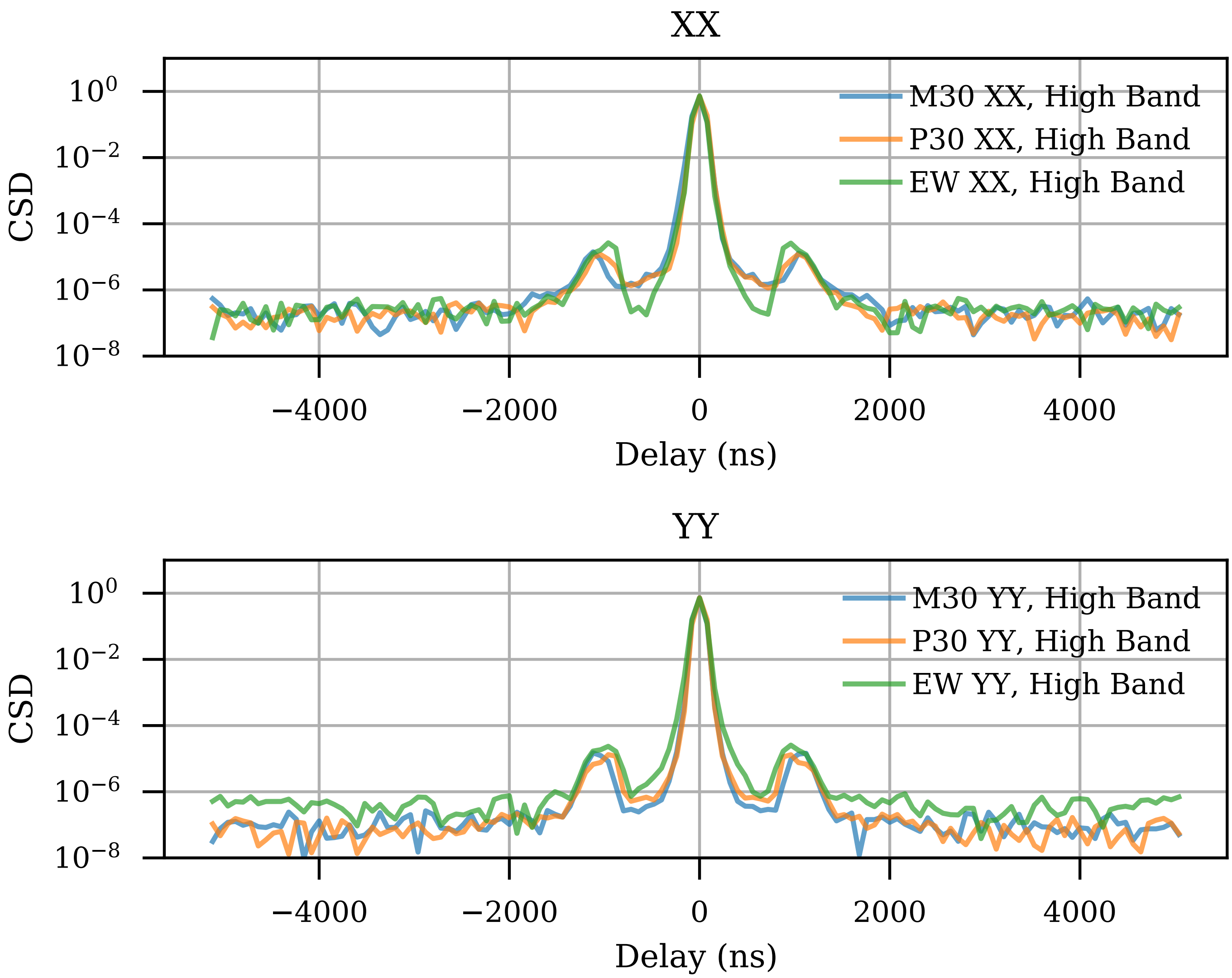

Figure 4: Delay transform of linear triads over a frequency band of 150-175MHz. CSD is the cross spectral power density, normalised on the unit circle.

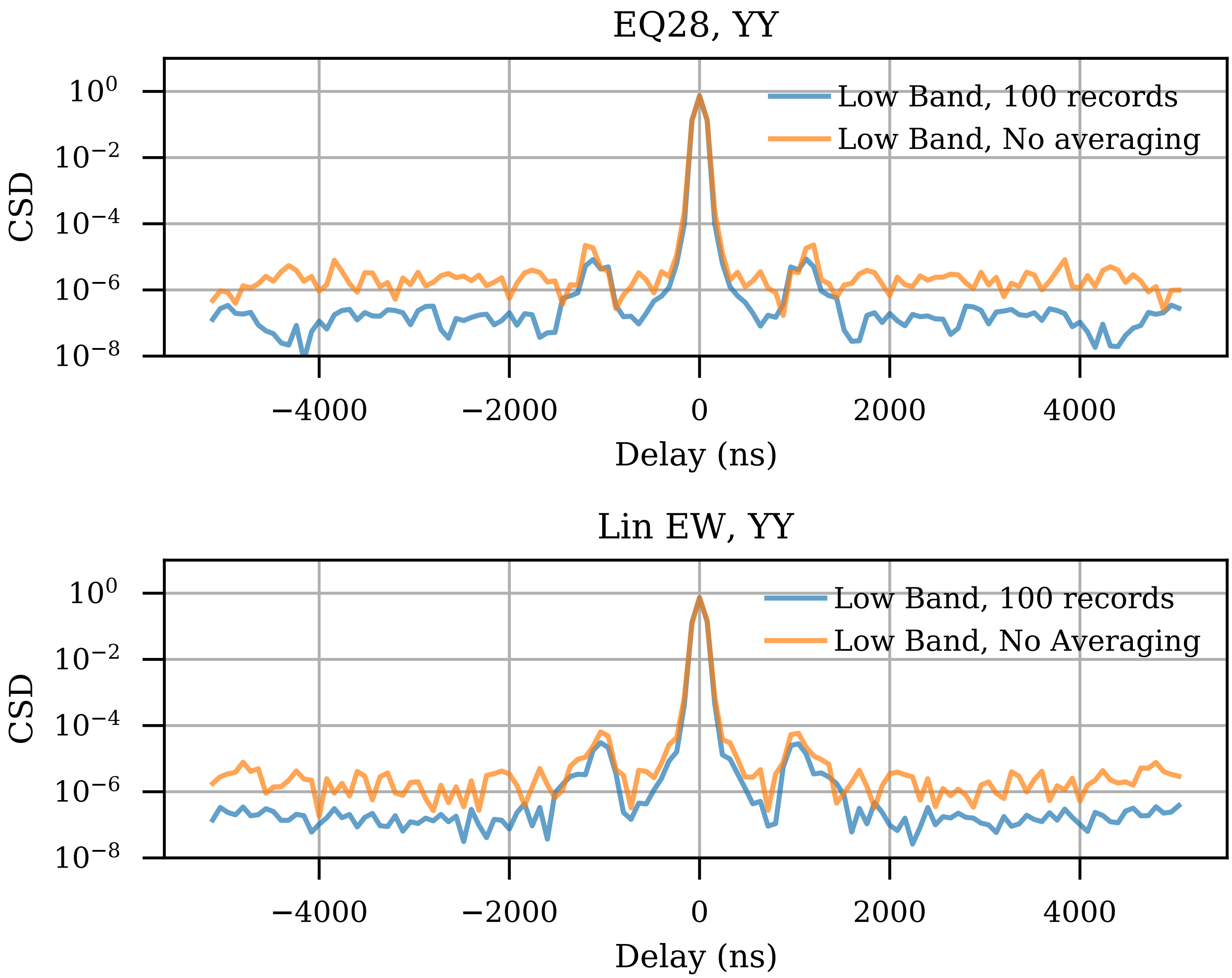

Figure 5: Delay transforms of EQ14 and LinEW triads showing the effects of averaging incoherently over 100 records versus the delay spectrum of a single record. Noise reduction is as expected.

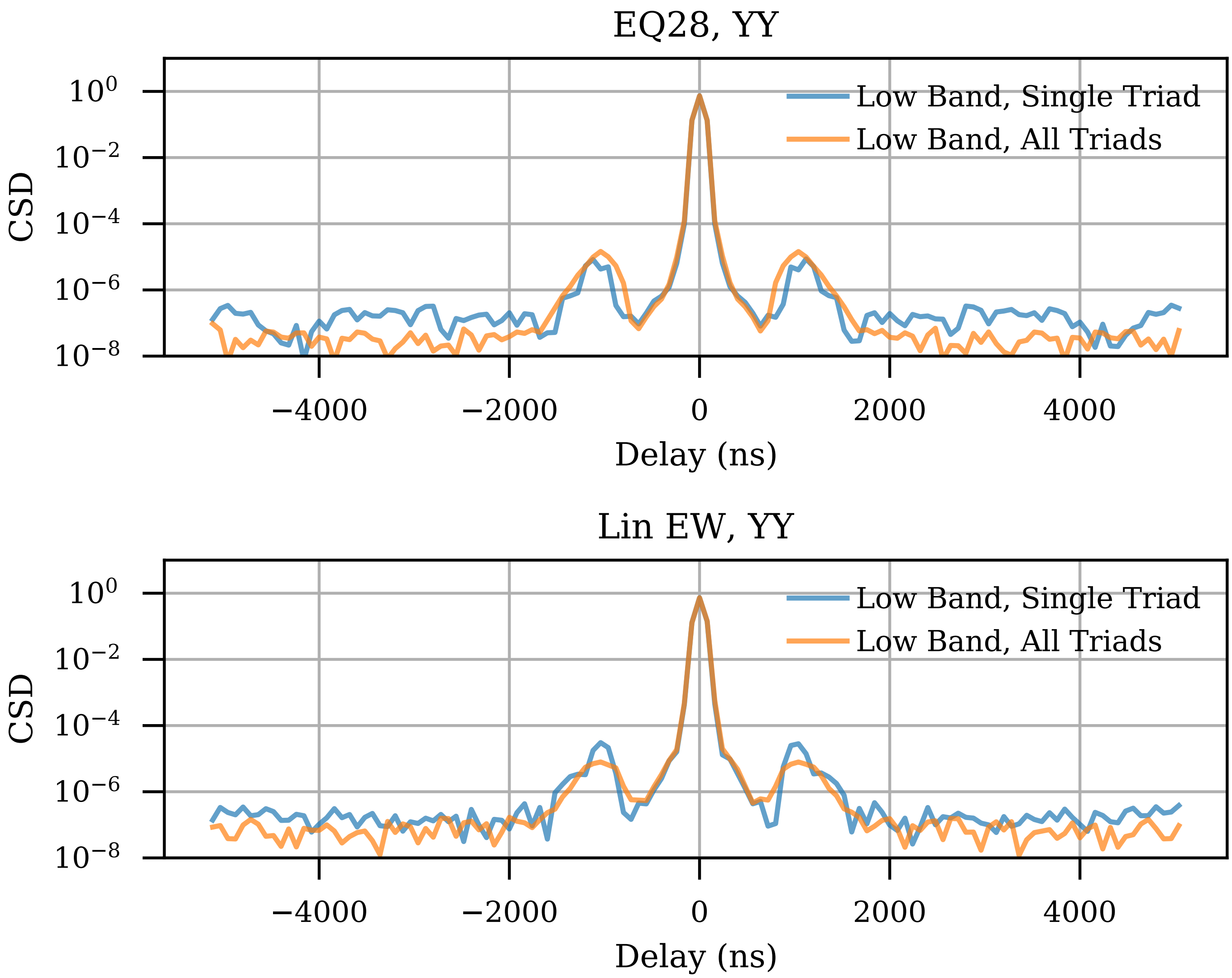

Figure 6: Same delay transforms as in 5, but with the addition of incoherent averaging over all triads. All plots are incoherently averaged over 100 records as in 5

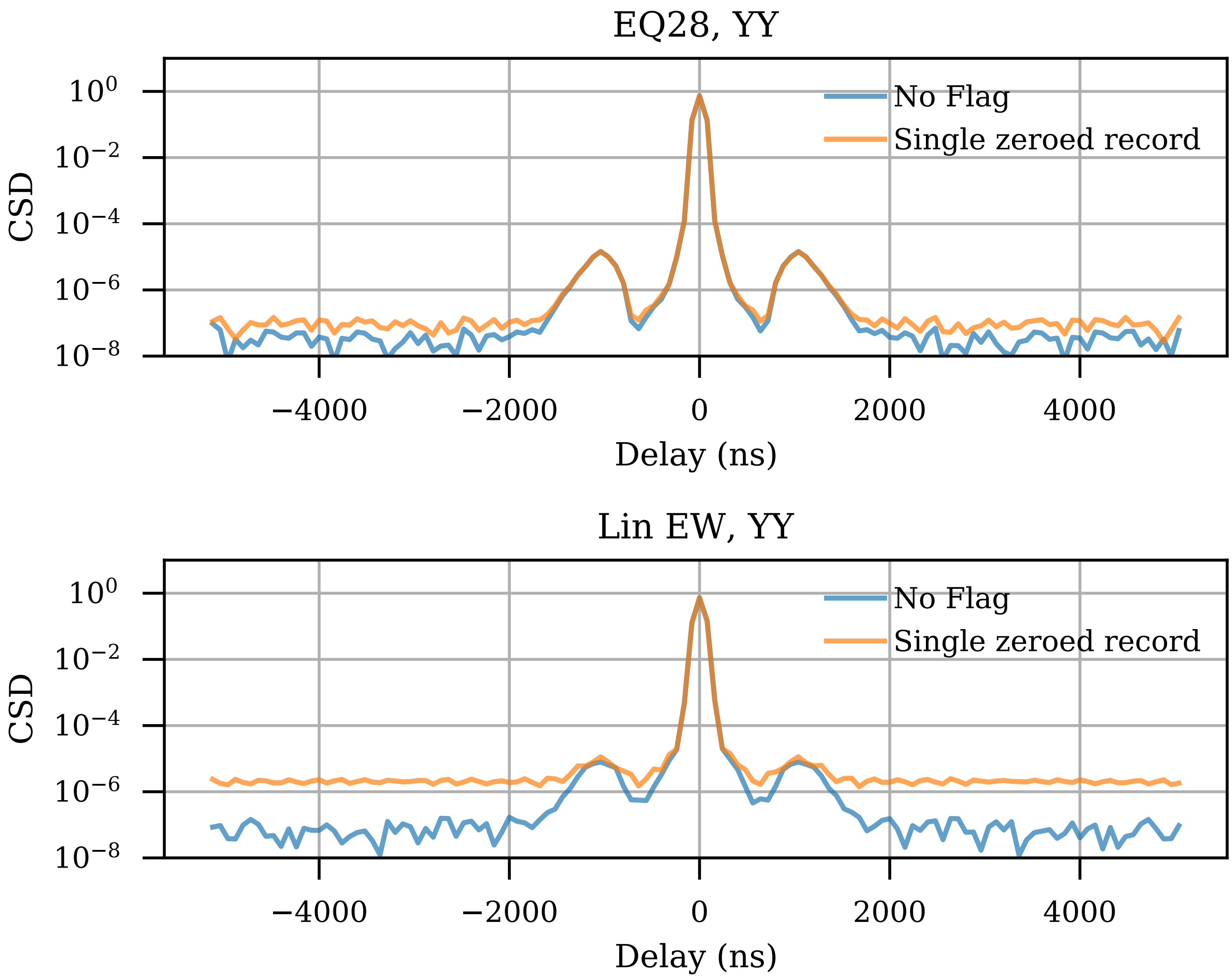

Figure 7: Delay transforms of our low band, but with the addition of a flagged (set to zero) channel for EQ14 and LinEW triads. The same channel is set to zero, with the difference between the two triad types is because of the average value of the closure spectrum at that point relative to zero. The LinEW zero channel causes a sharper impulse in the closure spectrum which translates into the higher noise floor in the delay spectrum.